AIAA JOURNAL
Vol. 36, No. 3, March 1998

Gasdynamical Detectors of Driver Gas Contamination in a High-Enthalpy Shock Tunnel

Norikazu Sudani*
National Aerospace Laboratory, Chofu, Tokyo 182-8522, Japan
and
Hans G. Hornung†
California Institute of Technology, Pasadena, California 91125

Simple gasdynamical devices consisting of a duct and a wedge have been applied to the detection of driver gas arrival in the test section of a high-enthalpy shock tunnel. Static pressure in the duct has been measured during a shot, and the time of driver gas arrival has been determined by the onset of the pressure rise, which indicates duct flow choking. The ability to detect driver gas in small concentrations is critical to the satisfactory performance of the device. Duct internal flows for various wedge angles have been numerically simulated to clarify the flow choking mechanism. The simulations give an idea of the improvement of detector sensitivity, and modified configurations of the detector are proposed. Flow visualization in the duct leads to a better understanding of pressure traces obtained, and pressure measurement data show a satisfactory degree of sensitivity. The arrival time of driver gas measured with the detectors is in good agreement with an analytical prediction based on a shock-bifurcation flow model. The useful test time in T5 with uncontaminated freestream is also demonstrated over a wide range of specific reservoir enthalpies.

Nomenclature

A_e = stream-tube area at the entry of the subsonic region
A_{exit} = area at the duct exit
A_{inlet} = area at the duct inlet
A_t = stream-tube area at the throat of the subsonic region
AR = aspect ratio of the duct inlet
h = duct height
h_0 = specific reservoir enthalpy
M = local Mach number
M_1 = Mach number at the duct inlet
M_∞ = freestream Mach number
p_{duct} = static pressure in the duct of the detector
p_0 = nozzle reservoir pressure
p_4 = burst pressure of the main diaphragm
w = duct width
x = distance from the reference point to the shock wave (see Fig. 10)
β = shock angle
γ = ratio of specific heats
θ_c = cone half-angle
θ_d = wedge angle at shock detachment
θ_{MR} = wedge angle at the transition from regular to Mach reflection
θ_w = wedge angle
θ_1 = angle of attack of the duct or angle of the shock generator

Introduction

In reflected shock tunnels, driver gas contamination is one of the most serious problems that limit the test time, especially for a high-enthalpy flow. The interaction between the reflected shock wave and the boundary layer on a shock tube wall causes bifurcation at the foot of the reflected shock. When the reflected shock is transmitted through the driver gas, the gas that passes through the bifurcation forms a jet along the wall towards the shock tube end and contaminates the test gas prematurely. Because a mixture of helium and argon is normally used as driver gas, the contamination of test gas by the monatomic driver gas leads to a change in gas composition and temperature in the test section flow, thereby influencing measurements in the chemically reacting flowfield.

The free-piston shock tunnel T5 (Ref. 1) at the Graduate Aeronautical Laboratories at the California Institute of Technology is a ground test facility capable of producing flows at high specific reservoir enthalpies to simulate hypervelocity reacting gas flows. The test duration determined by the constancy of reservoir pressure is only a few milliseconds. The driver gas contaminates the test gas earlier than the reservoir pressure falls, thus reducing further this short test time. Knowing when the driver gas arrives is therefore very important to determine the useful test time and to make reliable tests in such shock tunnels.

A simple flow model of the shock bifurcation[2] and extended works[3,4] have been reported, and test time predictions have also been proposed.[3,5] Until recently, however, no convenient experimental methods with a satisfactory degree of sensitivity (contamination level) and accuracy were established to detect the arrival time of driver gas in a test section and to validate the predictions. Although mass spectrometry[6,7] is considered the most suitable technique for the detection of low driver gas concentrations, the application of this technique to various shock tunnels is restricted by the size and complexity of the device. Thus, a simple diagnostic technique using gasdynamical effects is desirable to measure the contamination under various test conditions in each shock tunnel. The arrival time of the driver gas may not be repeatable because the contamination is attributed to intricate viscous and turbulent phenomena in the shock tube and its onset depends on the condition of the interface between driver gas and test gas.[5] It is desirable, therefore, that the detector be designed as small as possible for use in conjunction with other experimental models or be simple in construction so that it can be easily applied to the test section of shock tunnels when necessity arises.

For this purpose, Stalker[8] first proposed a probe-type device, which utilizes the difference of the ambient speed of sound between driver gas and test gas. Hornung et al.[9] detected the contamination onset by observing the behavior of the oblique shock over a wedge with a high-speed camera. In either case, however, the level of contamination detected was not sufficiently low. Olivier et al.[10] have

Presented as Paper 97-0561 at the AIAA 35th Aerospace Sciences Meeting, Reno, NV, Jan. 6–9, 1997; received May 24, 1997; revision received Oct. 31, 1997; accepted for publication Nov. 1, 1997.

*Senior Researcher, Aircraft Aerodynamics Division. E-mail: sudani@nal.go.jp. Member AIAA.

†Kelly Johnson Professor of Aeronautics and Director, Graduate Aeronautical Laboratories. Member AIAA.

Table 1 Gasdynamical duct detectors designed and tested in T5

Type	Inlet	Inclination, deg	Flow visualization
I	Axisymmetric	0	N/A
II	Square	0	N/A
III	Square	33	N/A
IV	Two dimensional ($AR = 12$)	33	Holographic interferometry

recently developed a method of detection using a static pressure probe. A different idea of a simple detector consisting of a square duct and a wedge has been proposed by Paull and King[11] to detect distinctly the arrival time of driver gas in a known concentration, and it was demonstrated that the experimental data were in good agreement with those from mass spectrometry. The principle is based on the fact that the angle of the shock wave emanating from the wedge in the duct increases with the arrival of monatomic driver gas because the ratio of specific heats becomes higher, assuming a calorically perfect gas. If both the location and the angle of the wedge are adjusted so that the duct internal flow does not choke for an uncontaminated test gas but does choke for a higher-γ gas, the driver gas arrival can be detected by an abrupt pressure rise indicating flow choking in the duct. Paull[12] used a wedge with an angle just below the shock detachment angle, thereby developing a detector with higher sensitivity. The detector configuration, however, has not been sufficiently optimized for satisfactorily high sensitivity and for the applicability to other shock tunnels or various test conditions.

On the basis of their idea, four detectors have been designed as shown in Table 1 and tested in T5. All of the detectors were instrumented with two piezoelectric pressure transducers separated along the flow direction to observe the behavior of the shock traveling upstream during the choking process. This paper first summarizes preliminary test results with the type I and II detectors and discusses the problem of detector sensitivity to a small amount of driver gas. To seek the optimum configuration of the detector, flows in the duct are numerically simulated for a calorically perfect gas, and the criterion for flow choking is clarified. This work led to a modified configuration, and experimental data acquired with the type III and IV detectors are presented, including flow visualization data. Measurements with the detectors have been made for different specific reservoir enthalpies to demonstrate useful test time over a wide range of enthalpies attainable in T5.

Experiments described in this paper were conducted at $p_4 = 32$ or 45 MPa and at specific reservoir enthalpies ranging from approximately 8 to 25 MJ/kg. The relatively low p_4 for T5 was selected in consideration of data productivity. Air was used as test gas except for a few cases with the type I detector, where N_2 was also used. All of the shots were made under the nearly tailored interface conditions.

Preliminary Tests

Axisymmetric Duct Detector

An axisymmetric duct detector (type I) with a cone was first designed as illustrated in Fig. 1 to avoid three-dimensional viscous effects occurring in the case of a square duct. Two different cone half-angles of 40 and 15 deg were chosen to examine the effect on detector sensitivity. The location of the cones is adjustable in the duct-axis direction.

Figure 2 shows pressure traces at both upstream and downstream locations in the duct for the two cone angles. The pressure change from before to after duct flow choking is distinguishable in each trace. This indicates that a certain amount of driver gas can be easily detected by the pressure measurement and that the gasdynamical method is basically applicable in T5. For $\theta_c = 40$ deg, however, the shock travels slowly upstream and the pressure rise during this choking process is accompanied by a large oscillation. This is attributed to the strong interaction between the shock and the boundary layer on the inner wall of the duct. In this case, the location of the pressure transducer is very critical to the detection of choking start, i.e., contamination onset. Furthermore, the pressure starts to rise gradually, so that the point of choking start is obscure.

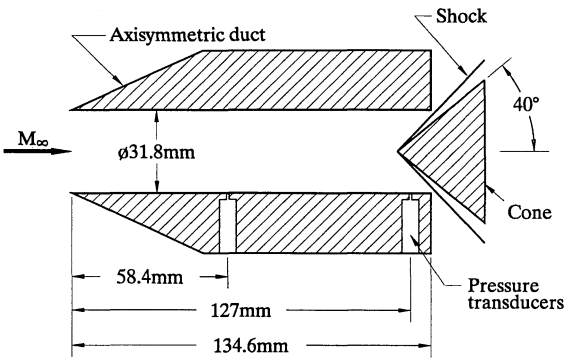

Fig. 1 Schematic of the axisymmetric duct detector (type I). The cone location is adjustable in the duct-axis direction.

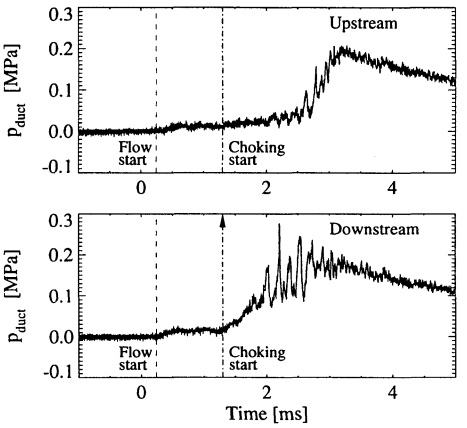

a) Shot # 985 (θ_c = 40 deg)

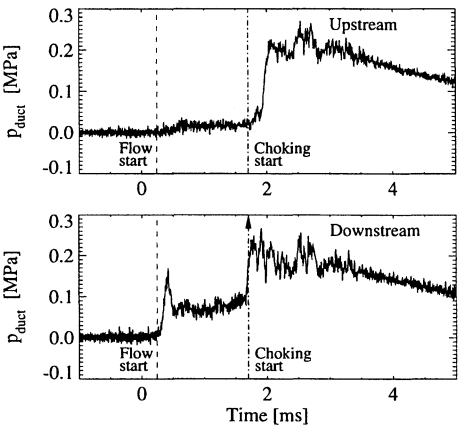

b) Shot # 998 (θ_c = 15 deg)

Fig. 2 Comparison of pressure traces with a large- and a small-angle cone in the axisymmetric duct detector (type I): $h_0 \simeq 20$ MJ/kg and $p_0 \simeq 12$ MPa.

For $\theta_c = 15$ deg, the shock generated by the cone is so weak that multiple shock reflections occur between the cone and the duct inner wall without flow choking. In contrast to the case of $\theta_c = 40$ deg, the shock travels upstream much faster, and the duct pressure rises steeply during choking. Thus, the determination of choking start is less dependent on the transducer location. For the type II, III, and IV detectors, pressure traces of the downstream transducer will be presented and discussed.

Square-Duct Detector

The aim of the axisymmetric model was to avoid unfavorable three-dimensional effects in the duct. No significant differences in the results were, however, recognized compared with those of the square duct presented by Paull and King[11] or Paull.[12] Furthermore, difficulty in adjusting cone location and concentricity arose during a series of the tests, and hence many shots were necessary for finding the proper cone position.

A smaller square-duct detector (type II) was then designed as illustrated in Fig. 3. Three detectors were used simultaneously in the test section to reduce the number of shots required for finding the proper wedge setup. The adjustment of wedge location was accomplished with accuracy of ±0.001 in. using a dial gauge. Either 10 or 20.5 deg was chosen for the wedge angle. For both angles, regular reflection of the wedge shock is expected to occur at the first reflection point on the wall.

Typical pressure traces for $\theta_w = 10$ deg are shown in Figs. 4b–4d, and one of the corresponding traces of nozzle reservoir pressure is shown in Fig. 4a. The reservoir pressure remains constant over a period of 2 ms because of nearly tailored interface operation. The flow in the duct, however, chokes because of contamination earlier than p_0 falls below 90% of the constant value. It can be seen that the driver gas contamination considerably reduces the useful test time. Figures 4b–4d show the effect of wedge location on choking time. If the wedge is placed downstream (Fig. 4b), the flow chokes late. This means that, in this setup, much driver gas is required for the duct to be choked. To make the detector most sensitive to a small amount of driver gas, the wedge must be placed just at the location upstream of which the duct is choked immediately after the flow start (Fig. 4d). Accordingly, approximately 1.1 ms, as shown in Fig. 4c, is regarded as the time when a small amount of driver gas reaches the test section.

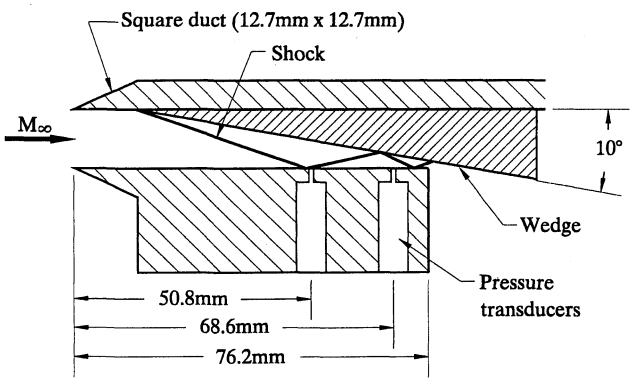

Fig. 3 Schematic of the square-duct detector (type II). The wedge location is adjustable in the duct-axis direction.

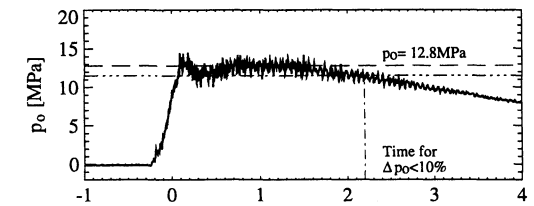

a) Shot # 1064 (nozzle reservoir pressure)

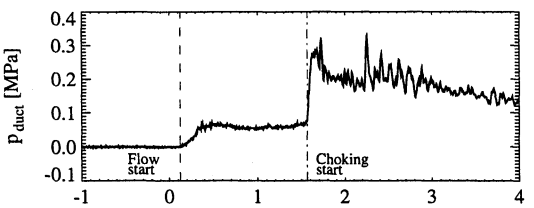

b) Shot # 1070 (A_{exit}/A_{inlet} = 0.132)

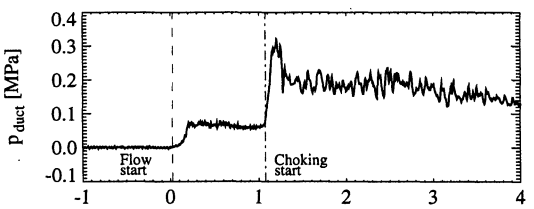

c) Shot # 1064 (A_{exit}/A_{inlet} = 0.123)

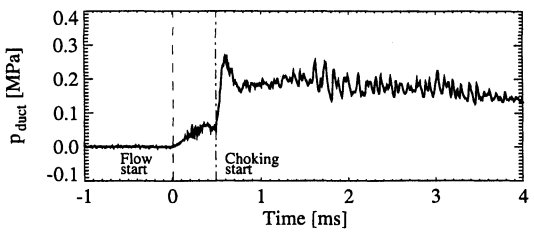

d) Shot # 1065 (A_{exit}/A_{inlet} = 0.113)

Fig. 4 Pressure traces in the square-duct detector (type II) for different exit area ratios A_{exit}/A_{inlet} and one of the corresponding traces of nozzle reservoir pressure: $h_0 \simeq 20$ MJ/kg and $\theta_w = 10$ deg.

Problems

The results of the preliminary tests yielded significant information on contamination in T5 for different specific reservoir enthalpies. However, the concentration of driver gas in the test section at the point of choking was uncertain. To determine whether or not the level of contamination detected is critical to experimental data obtained at that time or to simply know the detector performance, the detectors need to exhibit the detection threshold of driver gas contamination.

In the preliminary tests, the detectors were calibrated by deliberately seeding the test gas in the shock tube with driver gas as Paull and King[11] proposed. This produces a test gas contaminated by a known concentration of driver gas from the beginning of the flow. No satisfactorily repeated results, however, were obtained in T5. The cause is attributed to the increase in γ by the contamination of the test gas in the nozzle reservoir. The increase in γ leads to increased freestream Mach number, which decreases the oblique shock angle and has a negative effect on sensitivity. Accordingly, the wedge must be placed in the critical position for high sensitivity. In this situation, whether the duct "starts" or "unstarts" is very susceptible to the flow conditions, so that very slight changes of flow conditions during the unsteady nozzle starting process can cause the duct flow to choke. A number of shots are therefore needed for the detector to be adequately calibrated. This is impractical, especially for large facilities. Some modifications are necessary for high sensitivity so that the wedge can be located somewhat behind the critical position. In a simple theory, a large wedge angle yields better sensitivity. However, the problem of the strong shock/boundary-layer interaction, which causes obscure detection as shown in Fig. 2a, also needs to be solved in the modifications.

Numerical Simulations

To modify the detector, two-dimensional duct flows were numerically simulated in detail by using the Amrita computational system. Amrita is an acronym for adaptive mesh refinement interactive teaching aid and was conceived by Quirk (Ref. 13) as a means of automating computational fluid dynamics investigations right down to the level of constructing documents that explain both the purpose and the outcome of a particular study. The two-dimensional unsteady Euler equations were solved by using Roe's second-order flux-difference-splitting scheme with Harten's entropy fix, assuming a calorically perfect gas. Body-fitted grids were applied in these simulations. All of the results are presented in the form of pseudoschlieren images in which the gray shading is proportional to the magnitude of the density gradient. Sonic lines ($M = 1$) are superimposed as white lines. The application of Amrita to the Euler equations in this paper has not taken particular care to avoid numerical artifacts such as were pointed out by Quirk.[14] For example, Fig. 5a shows clear evidence of odd–even decoupling, which arises from the interaction of the shock with the grid in a way that results in a serrated shock. Also, in several places, difficulties arising from the problem of positivity preservation were avoided expediently by placing a double corner at the trailing edge of the wedge. Such artifacts can be eliminated or avoided more elegantly by suitable precautions, as has been discussed in detail by Quirk,[14] but in our application they do not affect the flows calculated to an extent that influences our argument.

Figure 5 shows simulations of duct internal flows with a wedge of which the angle is relatively large but smaller than the shock

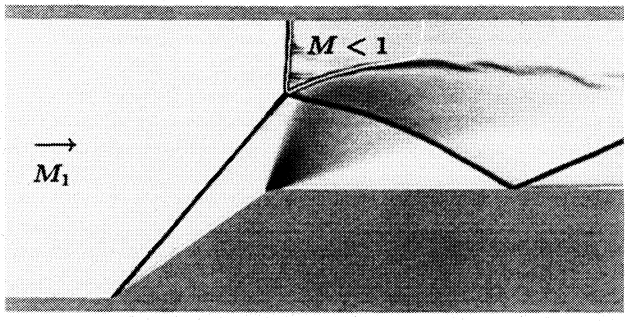

a) Unchoked (steady) flow

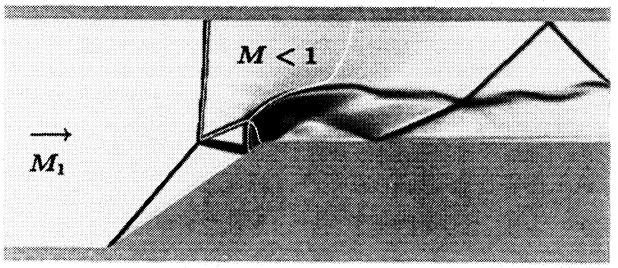

b) Choking flow for a smaller duct height

Fig. 5 Numerical simulations of duct internal flows with a wedge. Gray shading is proportional to the magnitude of density gradient, and sonic lines ($M = 1$) are superimposed as white lines: $M_1 = 5$, $\gamma = 1.4$, and $\theta_{MR} < \theta_w$ (35 deg) $< \theta_d$.

detachment angle. For the duct to be choked, two factors are required. One is a locally subsonic region produced by shock detachment from the wedge or by Mach reflection of the shock. The Mach reflection consists of three shocks, i.e., the incident shock, the reflected shock, and the Mach stem downstream of which the flow is subsonic.[15] As long as the wedge shock is attached and reflects in the form of regular reflection even several times, the duct flow never chokes. (Strictly speaking, it may choke if the flow is subsonic behind the last reflected shock with a sufficiently large angle.) The other is the contraction of the subsonic region. When the contraction ratio A_t/A_e becomes smaller than the limiting value by some disturbances or small duct-exit area, the flow in the duct is choked.[16] In Fig. 5a, the wedge shock is attached, and a Mach reflection occurs. Although another reflected shock appears, this shock does not impinge on the subsonic region behind the Mach stem. The duct flow is expected to be unchoked, and actually the shock wave configuration in Fig. 5a becomes stable after a sufficient number of computational time steps. If the duct height is smaller (Fig. 5b), the Mach stem length increases, and the reflected shock impinges on the inclined wedge wall. The second reflected shock then affects the subsonic region and reduces the throat area. The Mach stem should therefore be pushed upstream. Figure 5b illustrates a frame in the unsteady choking process with the Mach stem moving upstream.

In the case where the wedge shock is detached (Fig. 6), a subsonic region appears between the detached shock and the wedge inclined wall. When the Mach stem length is small (Fig. 6a), the subsonic region is free from disturbances, and then the duct flow remains unchoked despite the appearance of several subsonic pockets. For a smaller duct height (Fig. 6b), the Mach stem length becomes larger. The subsonic flow dominates the regions behind the Mach stem and the detached shock, thus leading to duct flow choking because of the small duct-exit area.

The results of the numerical simulations suggest that, if the wedge is high enough relative to the duct height, the flow chokes at the moment when a Mach reflection appears. For a small wedge angle, the shock can reflect several times between the wedge and duct walls without choking, and Mach reflection would occur at the last reflection. In this case, the criterion for choking is intimately related with the problem of the transition from regular to Mach reflection.[15] A wedge angle greater than that at the detachment condition for Mach reflection should be chosen so that the choking criterion is simply reduced to whether the first shock impinges on the opposite duct wall.

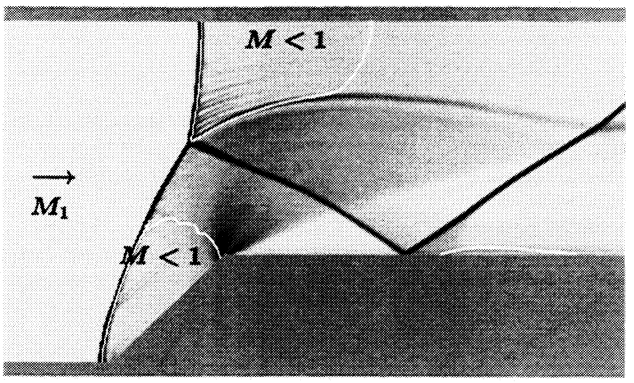

a) Unchoked (steady) flow

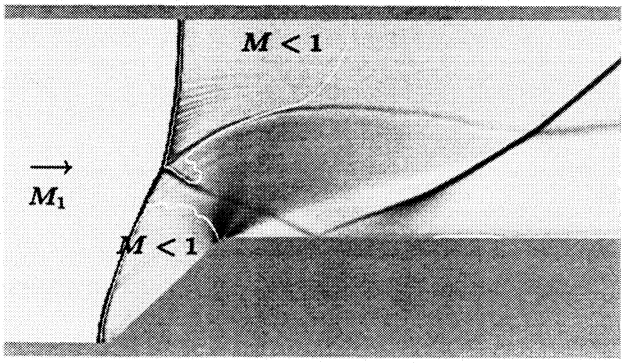

b) Choking flow for a smaller duct height

Fig. 6 Numerical simulations of duct internal flows with a wedge: $M_1 = 5$, $\gamma = 1.4$, and $\theta_d < \theta_w$ (44 deg).

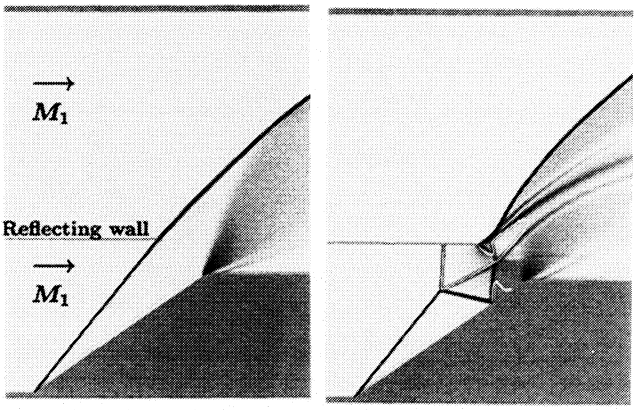

a) Unchoked (steady) flow for $\gamma = 1.44$

b) Choking flow for $\gamma = 1.45$

Fig. 7 Numerical simulations of flows around the end of the duct detector for different ratios of specific heats: $M_1 = 5$ and $\theta_{MR} < \theta_w$ (35 deg) $< \theta_d$.

Figure 7 simulates flow choking in the duct detector for different ratios of specific heats. For a lower γ (Fig. 7a), the wedge shock just misses the opposite duct wall, which is represented by a reflecting wall with zero thickness in this simulation. A slight increase in γ causes the shock to impinge on the wall and a Mach reflection to occur (Fig. 7b). Because the wedge is high enough for the second reflected shock to form and affect the subsonic region, the flow starts to choke the moment the shock impinges.

Tests with Modified Detectors

Modification of the Detector

Numerical simulations suggest that both the angle and the location of the wedge be adjustable to attain high sensitivity as shown in Fig. 8. Making both adjustments, however, is impractical because of the enormous increase in the number of shots required. The variable wedge angle gives the greatest increment of the shock angle near detachment. However, in relation to the choking criterion, the shock

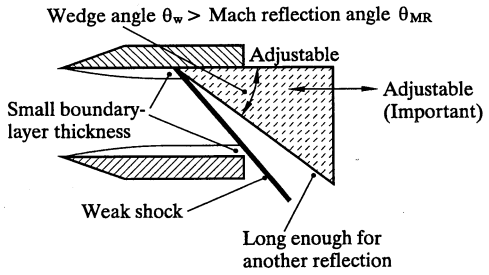

Fig. 8 Optimization of the duct detector for high sensitivity to a small concentration of driver gas.

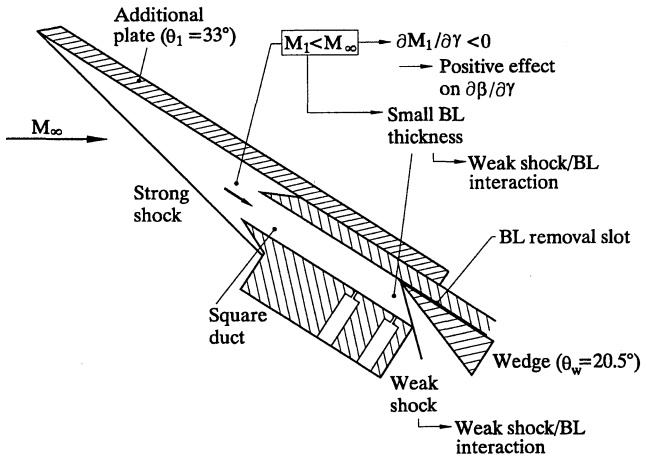

Fig. 9 Modified configuration of the square-duct detector (type III).

detachment from the wedge tip is not critical. The adjustment of the wedge location is more essential and directly relates to sensitivity because the shock should impinge on the duct wall at the driver gas arrival time. Thus, the wedge angle does not need to be variable if it is greater than θ_{MR}. Adopting this relatively large angle, however, requires reduction of the interaction between the wedge shock and the boundary layers in the duct.

Figure 9 illustrates a modified configuration (type III) of the square-duct detector for higher sensitivity and for weak shock/boundary-layer (BL) interaction. A flat plate is attached to the outer wall of the square duct, and both are installed at a relatively high angle of attack to the freestream. A simple calculation shows that, when the angle of attack of the flat plate is greater than approximately 15 deg, driver gas contamination causes the Mach number behind the oblique shock to decrease despite the fact that it increases the freestream Mach number. The change in duct inlet Mach number yields a positive effect on sensitivity in contrast to the case of the detector without inclination. The inlet Mach number is approximately 2 under typical conditions in T5 ($M_\infty \simeq 5$), and the unit Reynolds number of the duct flow is almost the same as the freestream Reynolds number. Because of this low Mach number at the same Reynolds number, the boundary layers in the duct should be thinner[17] and the wedge shock weaker. In addition, the wedge is placed a short distance away from the inside wall to avoid the boundary-layer influence. Much weaker interaction between the shock and the boundary layers is therefore expected in this modified configuration. A numerical simulation at $M_1 = 2$ shows that the duct flow chokes when a wedge shock with a large angle impinges on the duct wall, as in the case of $M_1 = 5$. This is because the duct exit is too small to let all the subsonic flow behind the Mach stem and the first reflected shock pass through.

When θ_w is greater than θ_{MR}, the necessary amount of the wedge shock movement toward the duct end for impingement determines the sensitivity of the detector. In this case, the sensitivity is proportional to the effect of γ on the shock position x, thereby being represented by $-(\partial x/\partial \gamma)$. Figure 10 shows results of a sensitivity analysis with a fixed h for a calorically perfect gas. The calculation includes the change in M_∞ caused by the increase in γ. The lowest thick line is for the duct without inclination ($\theta_1 = 0$ deg). As the duct is inclined to the freestream, the sensitivity improves markedly.

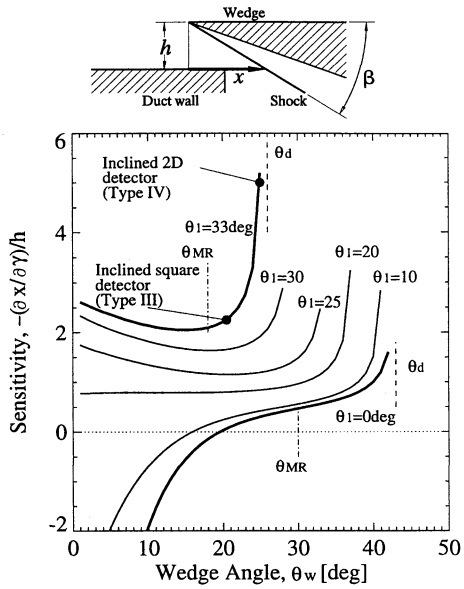

Fig. 10 Sensitivity of duct detectors with and without inclination. This calculation includes the change in freestream Mach number caused by the increase in γ.

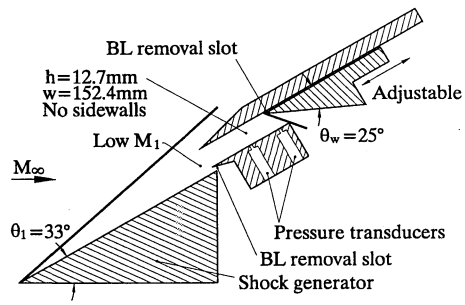

Fig. 11 Two-dimensional duct detector (type IV) allowing flow visualization of duct internal flow.

The modified configuration is expected to be applicable to various test conditions with high sensitivity by properly selecting the best combination of θ_1 and θ_w.

Another modified detector (type IV) was designed as illustrated in Fig. 11 to visualize the duct internal flow for a better understanding of pressure traces. The duct is 0.5 in. high and 6 in. wide without sidewalls. A couple of pressure transducers are installed in the spanwise direction to check the two-dimensionality. This detector is also expected to yield a decrease in the number of shots required for the adjustment of the wedge location.

In the modified configurations, an angle of shock generator of 33 deg was chosen, and wedge angles were fixed at 20.5 and 25 deg for the type III and IV detectors, respectively. The location of the wedges was adjusted in the duct-axis direction. These experimental design points are also plotted in Fig. 10, where the type IV detector appears to be very close to the best configuration for test conditions in T5.

Results and Discussion

Figure 12 shows pressure traces for the inclined square-duct detector (type III) at a specific reservoir enthalpy of 25 MJ/kg, which is the highest attainable in T5. The phrases 12.5% He + Ar and 25% He + Ar denote the mole fraction of monatomic driver gas with which test gas was deliberately seeded in the shock tube for calibrations of the detector. The mixture ratio of helium and argon was determined so that the incident shock speed was unchanged. For an unseeded test gas (0% He + Ar), the flow starts to choke at 1.6 ms, whereas it chokes immediately after the flow reaches the duct for a test gas seeded with 25% of driver gas. This indicates that the detector is set to be choked for mixtures with 25% of driver gas. It is therefore possible that 25% or less of driver gas reaches the test section at 1.6 ms. Similarly, from the trace for a test gas seeded with

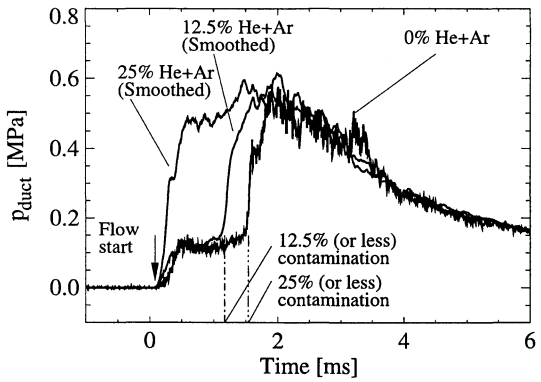

Fig. 12 Pressure traces in the modified square-duct detector (type III) at a high specific reservoir enthalpy for an unseeded test gas and driver gas seeded test gases: $h_0 \simeq 25$ MJ/kg and $p_0 \simeq 20$ MPa.

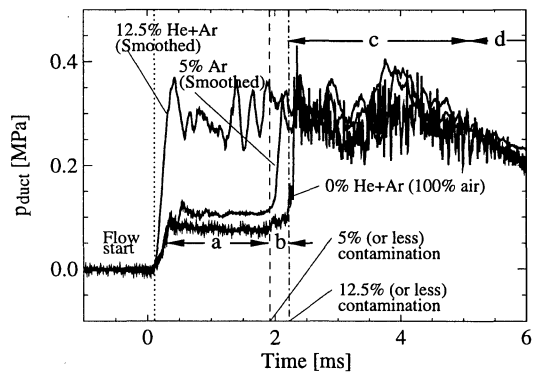

Fig. 13 Pressure traces in the two-dimensional duct detector (type IV) at a moderate specific reservoir enthalpy for an unseeded test gas and driver gas seeded test gases: $h_0 \simeq 14$ MJ/kg and $p_0 \simeq 15$ MPa.

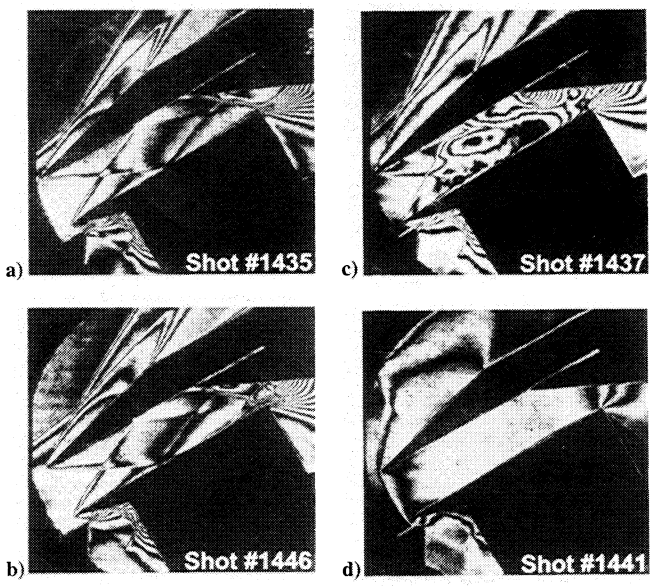

Fig. 14 Holographic interferograms of duct internal flows. Each picture qualitatively corresponds to the part of the pressure trace with the same label in Fig. 13: $h_0 \simeq 14$ MJ/kg and $p_0 \simeq 15$ MPa.

12.5% of driver gas, it can be seen that 12.5% or less of driver gas additionally arrives at the test section at approximately 1.2 ms.

A moderate h_0 was selected for measurements with the inclined two-dimensional detector (type IV) because the period of unchoked (uncontaminated) flow is expected to be so long that experimental data obtained can rather easily be interpreted. Pressure traces for an unseeded test gas and deliberately seeded test gases are shown in Fig. 13, and holographic interferograms of the duct internal flow for an unseeded test gas are shown in Fig. 14. The pictures were taken in different shots, for which the detector setup was not exactly the same, but each picture qualitatively corresponds to the part of the pressure trace with the same label. The flow patterns in the duct fall into four categories.

1) In the category of uncontaminated and unchoked flow (period *a* in Figs. 13 and 14a), the wedge shock does not impinge on the duct inner wall, and hence the flow in the duct is unchoked and everywhere supersonic. The pressure in the unseeded case is not affected by the presence of the wedge shock, thus being nearly equal to the static pressure of the outer flow. This period is considered useful test time with uncontaminated freestream.

2) In the category of slightly contaminated but unchoked flow (period *b* in Figs. 13 and 14b), when the angle of the wedge shock is increased, an interaction between the wedge shock and the boundary layer on the duct inner wall is observed. It thickens the boundary layer near the end of the duct, but the flow is unchoked because no reflection of the shock occurs. The pressure for the unseeded test gas indicates a slight rise caused by the influence of the wedge shock on the duct wall boundary layer. Similarly, for a test gas seeded with 5% of monatomic gas, the pressure before choking is slightly higher than that of the unseeded case. It is therefore possible that the flow is contaminated by 5% or less of driver gas during this period.

3) In the category of contaminated but incompletely choked flow (period *c* in Figs. 13 and 14c), when the shock angle is further increased by a certain amount of driver gas, the shock impinges on the duct inner wall and then starts to travel upstream. Because subsonic flow behind the traveling shock can spill from the duct because it has no sidewalls, the shock stays in the duct. (Actually it might be moving slowly upstream.) However, the shock moves very fast to the point where it comes to rest, so that the pressure shows an abrupt rise. As long as pressure transducers are located near the duct end, they can detect the shock motion, so that the dependency of their location on the detection of the pressure rise onset is considered negligibly small. For a test gas seeded with 12.5% of monatomic gas, this type 3 flow is observed immediately after the flow reaches the duct. This means that 12.5% or less of driver gas contaminates the test gas at the time of the abrupt pressure rise in the case of the unseeded test gas.

4) In the category of contaminated and fully choked flow (period *d* in Figs. 13 and 14d), when much driver gas reaches the duct, the shock travels upstream farther to be detached in front of the duct. The duct internal flow is everywhere subsonic and fully choked. Because no shock waves exist in the duct, the pressure trace is not as noisy as the trace during period *c*.

The measurement error of the duct detector technique was roughly estimated under some simple assumptions. The error depends on the repeatability of freestream properties. Some variation in freestream properties from shot to shot is mainly caused by that in p_4 or incident shock speed. A quasi-one-dimensional nonequilibrium nozzle flow calculation with measured data gives the freestream Mach number and the chemical composition. It also gives the ratio of specific heats assuming a chemically and vibrationally frozen flow. The necessary amount of driver gas for the shock to impinge on the duct end therefore is not exactly the same for each shot because the shock angle before the contamination is slightly different. The repeatability of the shock angle influences the accuracy of the detector. The freestream variability translates into an equivalent variability of driver gas concentration of $\pm 3\%$ by volume at a high enthalpy ($h_0 \simeq 20$ MJ/kg) and $\pm 1\%$ at a low enthalpy ($h_0 \simeq 8$ MJ/kg). Furthermore, the estimation with a practical value of wedge adjustment shows that an inclined-duct detector is capable of attaining sensitivity to 5% of driver gas, whereas a detector without inclination is 20%. The best sensitivity was attained with the type IV detector by means of careful adjustments with the aid of flow visualization data. Both the error and the sensitivity estimated are substantially comparable to those attained by mass spectrometry.[7]

Useful Test Time in T5

All of the experimental data measured with the duct detectors in T5 are plotted as functions of specific reservoir enthalpy in Fig. 15. The origin of the time axis in this figure corresponds to the time when flow reaches the test section, i.e., when the pressure in the duct starts to rise. The time therefore includes a period until the steady flow is

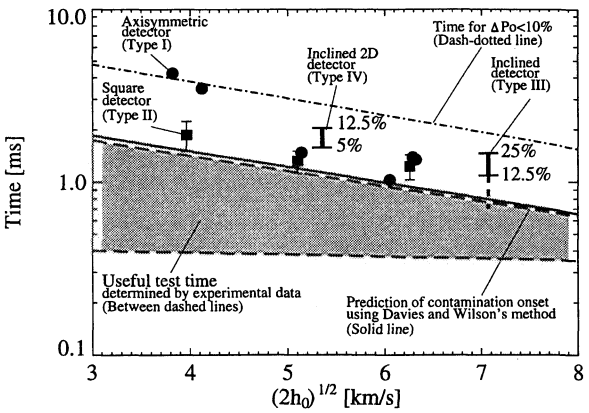

Fig. 15 Useful test time with uncontaminated freestream determined by the experimental data with duct detectors in T5 and a comparison with a prediction based on a simple shock-bifurcation flow model. Note the late choking of the type IV detector at intermediate enthalpy. This is thought to be related to slightly off-tailored interface operation.

established in the duct and is represented by the lower dashed line. The upper dashed line is derived from the earliest choking time for each enthalpy ($h_0 \simeq 8$, 13, 20, or 25 MJ/kg). The contamination occurs earlier than the time at which p_0 drops by 10% of its nearly constant value irrespective of h_0 (denoted by a dash–dotted line). Thus, the shaded region between the two dashed lines is defined as the useful test time with uncontaminated freestream. The contamination onset is predicted by Davies and Wilson's method[3] based on a simple shock-bifurcation model (a solid line) using measured values for the incident and reflected shock speeds. This is in excellent agreement with the upper dashed line. Davies and Wilson's method gives a reliable prediction of the early contamination onset for a wide range of enthalpies in T5.

The two-dimensional duct detector (type IV), once properly adjusted and calibrated, provided the best detection of very small concentrations of driver gas. Nevertheless, as shown in Fig. 15, the result indicates somewhat later time of the contamination onset than the predicted value or the other experimental values at the same enthalpy. This is thought to be related to the condition of the interface between driver gas and test gas after the reflected shock passes through the interface. Numerical simulations performed by Chue and Itoh[18] showed that the driver gas jet along the shock tube wall was severe at the tailored and overtailored interface operations (where the incident shock Mach number was greater than the tailored interface value), whereas the jet was too weak to transport the driver gas toward the shock tube end at undertailored interface operations (where the incident shock Mach number was smaller than the tailored interface value). Despite the fact that much attention was paid to tailoring in a series of the tests, very slightly off-tailored (under- or overtailored) interface operations might result in the scatter of the time detected. The effect of interface condition on the early contamination must be experimentally examined to optimize the useful test time for each test condition.

Conclusions

Simple gasdynamical duct detectors for the contamination of test gas by monatomic driver gas have been designed on the basis of Paull and King's[11] idea and tested in T5. The detectors installed with no inclination to the freestream do not exhibit satisfactorily high sensitivity and good repeatability. Numerical simulations clarify flow choking in a duct with a wedge and provide a hint for developing a highly sensitive detector. Some modifications produce sensitivity to 5% by volume of driver gas by utilizing low Mach number flow behind a strong oblique shock. Flow visualization data in the duct give a better understanding of pressure traces and the reduction of the number of shots required for finding the best detector setup. The sensitivity of the gasdynamical detector is comparable to more elaborate methods, e.g., mass spectrometry, for the detection of helium (and/or argon) arrival. The detector is expected to be suitable for initial measurements for determining the useful test time of shock tunnels because of its applicability to various test conditions, the simplicity of the device, and low cost. Although it might be difficult to use the modified detector routinely in conjunction with other experimental models, it can be put in the test section easily and frequently to check the test time for a different test condition. It is also possible that some experimental models with high-incidence windward sections may allow the modified configuration to be applied simultaneously.

The contamination data in T5 have been acquired over a wide range of specific reservoir enthalpies. The experimentally determined relation between h_0 and the useful test time is in good agreement with the prediction using Davies and Wilson's analytical method. The information of the driver gas contamination is helpful to decide the period during which quantitative measurements and flow visualization should be performed. Furthermore, it is valuable to the estimation of test time when the same type of shock tunnel is newly designed.

Acknowledgments

The authors would like to thank James J. Quirk of the California Institute of Technology for providing the Amrita computational system and his technical advice. They are also grateful to Bahram Valiferdowsi and graduate students in the T5 group for their help in performing the experiments.

References

[1]Hornung, H. G., "Performance Data of the New Free-Piston Shock Tunnel at GALCIT," AIAA Paper 92-3943, July 1992.

[2]Mark, H., "The Interaction of a Reflected Shock Wave with the Boundary Layer in a Shock Tube," NACA TM1418, March 1958.

[3]Davies, L., and Wilson, J. L., "Influence of Reflected Shock and Boundary-Layer Interaction on Shock-Tube Flows," *Physics of Fluids*, Supplement 1, 1969, pp. I-37–I-43.

[4]Matsuo, K., Kawagoe, S., and Kage, K., "The Interaction of a Reflected Shock Wave with the Boundary Layer in a Shock Tube," *Bulletin of the Japan Society of Mechanical Engineers*, Vol. 17, No. 110, 1974, pp. 1039–1046.

[5]Stalker, R. J., and Crane, K. C. A., "Driver Gas Contamination in a High-Enthalpy Reflected Shock Tunnel," *AIAA Journal*, Vol. 16, No. 3, 1978, pp. 277–279.

[6]Slade, J. C., Crane, K. C., and Stalker, R. J., "Driver Gas Detection by Quadrupole Mass Spectrometry in Shock Tunnels," *Shock Waves @Marseille, Proceedings of the 19th International Symposium on Shock Waves*, Vol. 1, Springer–Verlag, Berlin, 1995, pp. 293–298.

[7]Skinner, K. A., and Stalker, R. J., "Time-of-Flight Mass Spectrometer for Impulse Facilities," *AIAA Journal*, Vol. 32, No. 11, 1994, pp. 2325–2328.

[8]Stalker, R. J., "A Driver Gas Contamination Probe for Shock Tunnels," *Aeronautical Quarterly*, Vol. 19, May 1968, pp. 183–191.

[9]Hornung, H., Sturtevant, B., Bélanger, J., Sanderson, S., Brouillette, M., and Jenkins, M., "Performance Data of the New Free-Piston Shock Tunnel T5 at GALCIT," *Proceedings of the 18th International Symposium on Shock Waves*, Springer–Verlag, Berlin, 1992, pp. 603–610.

[10]Olivier, H., Kindl, H., Zhao, H., Muylaert, J., Wong, H., and Walpot, L., "Conventional Flow Diagnostics in Shock Tunnels," *Proceedings of the 21st International Symposium on Shock Waves* (to be published).

[11]Paull, A., and King, M. D., "A Driver Gas Detection Device for Shock Tunnels," *Shock Waves*, Vol. 4, No. 5, 1995, pp. 289–291.

[12]Paull, A., "A Simple Shock-Tunnel Driver-Gas Detector," *Proceedings of the 20th International Symposium on Shock Waves*, Vol. 2, World Scientific, Singapore, 1996, pp. 1557–1562.

[13]Quirk, J. J., "Amrita—A Computational Facility for CFD Modelling," VKI 29th CFD Lecture Series, von Kármán Inst. for Fluid Dynamics (to be presented).

[14]Quirk, J. J., "A Contribution to the Great Riemann Solver Debate," *International Journal for Numerical Methods in Fluids*, Vol. 18, No. 6, 1994, pp. 555–574.

[15]Hornung, H., "Regular and Mach Reflection of Shock Waves," *Annual Review of Fluid Mechanics*, Vol. 18, 1986, pp. 33–58.

[16]Seddon, J., and Goldsmith, E. L., *Intake Aerodynamics*, AIAA Educational Series, AIAA, Washington, DC, 1985, pp. 150–152.

[17]Anderson, J. D., Jr., *Hypersonic and High Temperature Gas Dynamics*, McGraw–Hill, New York, 1989, pp. 242–244.

[18]Chue, R. S. M., and Itoh, K., "Influence of Reflected-Shock/Boundary-Layer Interaction on Driver-Gas Contamination in High-Enthalpy Shock Tunnels," *Proceedings of the 20th International Symposium on Shock Waves*, Vol. 1, World Scientific, Singapore, 1996, pp. 777–782.

G. Laufer
Associate Editor